

Measurement of the Rigidity Coefficients of a Melamine Foam

N. Geebelen, L. Boeckx, G. Vermeir, W. Lauriks

Laboratorium voor Akoestiek en Thermische Fysica, Katholieke Universiteit Leuven, Celestijnenlaan 200D, 3001 Heverlee, Belgium

Jean F. Allard, Olivier Dazel

Laboratoire d'Acoustique de l'Université du Maine, Avenue Olivier Messiaen, 72000 Le Mans, France

Summary

For an isotropic elastic solid, all the rigidity coefficients can be evaluated from the velocities of the shear wave and of the compressional wave. For an isotropic porous frame, the rigidity coefficients of the frame in vacuum can be evaluated from the velocities of the frame compressional Biot wave and the shear Biot wave when the porous frame is saturated by air. The velocity of the frame compressional Biot wave is evaluated at audible frequencies from the detection of the quarter compressional wavelength resonance generated with a point source in air for samples bonded on a rigid impervious backing. In a previous work, the second measured parameter was the velocity of the shear wave evaluated from the quarter shear wave resonance. In this work, the second parameter is the velocity of the Rayleigh waves slightly modified by the finite thickness of the samples, the observation of the shear resonances being difficult for the melamine foam.

PACS no. 43.20.Gp, 43.20.Jr, 43.20.Ye

1. Introduction

For an isotropic elastic solid, all the rigidity coefficients are known when the values of two independent parameters, for instance the Poisson coefficient and the shear modulus, are known. For an isotropic elastic porous medium, the stress-strain relations in the context of the Biot theory [1, 2, 3] involve two independent parameters for the porous frame in vacuum and two other parameters, the bulk modulus of the material from which the frame is made and the bulk modulus of the saturating fluid. For usual air saturated sound absorbing porous media like reticulated foams, the bulk modulus of the material from which the frame is made is generally much larger than the bulk modulus of the porous frame and of the air and this material can be considered as an incompressible medium. The bulk modulus of the air in the porous medium can be predicted. The rigidity coefficients of the frame in vacuum play an important role in the prediction of sound transmission through layered porous materials. Many methods [4, 5, 6, 7] can be used to measure at low frequencies the rigidity parameters of the frames of porous sound absorbing media in vacuum. At audible frequencies, other methods can be used, based on the properties of the Rayleigh wave or the different surface modes and bulk modes of the porous structures [8, 9, 10]. The Biot theory can de-

scribe these modes and their excitation by a source in air or at the surface of the layer [11, 12] with a good precision. The bulk modes and the surface modes of the frame of a reticulated foam in air are not very different from the same modes in vacuum and in a first approximation the properties of the Rayleigh wave in an isotropic solid can be transposed without strong modifications when the solid is replaced by a porous structure. The rigidity coefficients and the density of the solid can be replaced in a first approximation by the elastic coefficients and the density of the porous frame. The main difference lies in the orders of magnitude of the celerity of the Rayleigh wave, between 50 m/s and 100 m/s for usual reticulated foams. A second difference is the large loss angle of the elasticity coefficient of the porous frames, around 0.1 for the reticulated foams, which induces a large damping of the Rayleigh wave. A third difference is the light dispersion due to the dependence of the rigidity coefficients of the porous structure on frequency. Recently, the evaluation of the rigidity coefficients of an urethane foam in vacuum has been performed from the observation of compressional and shear wave resonances generated by a point source in air [13]. Two different configurations have been considered: the porous layer bonded onto a rigid impervious backing and free on both faces. The geometry of the experiment is represented in Figure 1. The height of the point source S is h . The velocity is measured at M with a laser vibrometer. The radial distance from the source S to M is r . The vertical and the horizontal displacement have been predicted and measured to

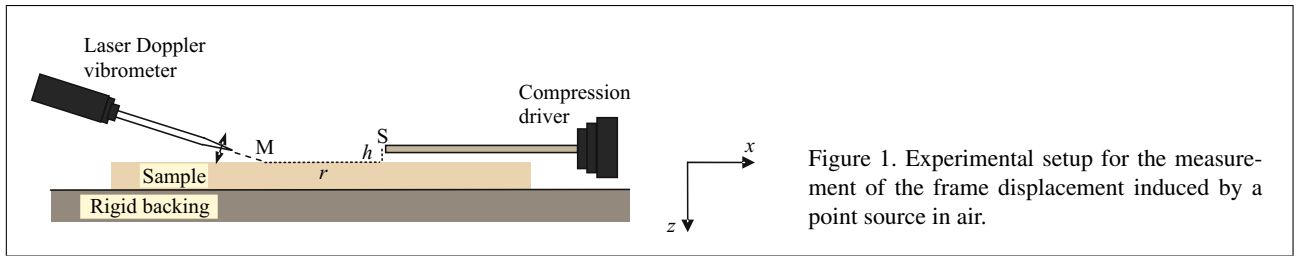


Figure 1. Experimental setup for the measurement of the frame displacement induced by a point source in air.

set in evidence the shear and the compressional resonances of the frame. Preliminary measurements on a melamine foam have shown that for this material only the detection of the compressional mode in the first configuration was easy. Some reasons for the difficulties concerning the detection of the shear resonances are suggested at the end of section II and of section IV. In this work, the quarter compressional wavelength resonance is detected for two layers of different thicknesses, $l = 2$ cm and $l = 5$ cm. The information provided by the quarter compressional wavelength resonance which can be detected for the first configuration is not sufficient to evaluate two independent rigidity coefficients in vacuum, for instance the shear modulus and the Poisson coefficient, of the melamine frame considered as an isotropic medium. Measurements of the velocity of the Rayleigh waves are performed to complete the information. The modification of the velocity of the Rayleigh wave due to the finite thickness of the samples is taken into account. The experimental set for the generation and the observation of the Rayleigh wave at audible frequencies, as described in section IV, is adapted to a restricted category of materials, the reticulated porous foams having a soft structure and therefore a small phase velocity of the Rayleigh wave. It may be noticed that the Rayleigh wave has not been observed on glass wools which have also a soft porous structure. Similarly, the observation of a quarter wavelength resonance at audible frequencies with samples having a thickness of several cm is possible only if the celerity of the compressional wave is sufficiently small, with an order of magnitude of 100 m/s.

2. Frame displacement induced by a point source in air

In a first step, the Biot theory [1, 2, 3], with the formalism developed in reference [3], is used to predict the plane wave reflection coefficient R , and the horizontal and the vertical displacement components u_x and u_z of the porous frame created at the surface of the layer by a plane wave in air with an horizontal wave number $k_x = \xi$ (The axes x and z are represented in Figure 1). The model by Johnson *et al.* [14] is used to describe the viscous and the inertial interactions, and the model by Lafarge [15] is used for the bulk modulus of the saturating air. These models use three traditional parameters, porosity, tortuosity and flow resistivity. Three other parameters are used, the thermal permeability, defined by Lafarge [15], describes at low frequencies the thermal exchanges between the frame and the air,

and the characteristic dimensions describe at high frequencies the viscous interaction [14] and the thermal exchanges [3]. The use of these models in the Biot theory is described in the Appendix. The angle of incidence θ related to ξ is defined by

$$\sin \theta = \xi/k, \tag{1}$$

where k is the wave number in the free air. A description of this first step is given in reference [13]. In a second step, the Sommerfeld representation [16] of a unit monopole pressure field in air is used to evaluate the normal velocity \dot{U}_z and the radial velocity \dot{U}_r of the frame created at the surface of the layer by the unit source at a height h and at radial distance r

$$\dot{U}_z(r) = i \int_0^\infty \frac{\xi d\xi}{\mu} (1 + R(\xi)) \exp(i\mu h) J_0(\xi r) u_z(\xi), \tag{2}$$

$$\dot{U}_r(r) = - \int_0^\infty \frac{\xi d\xi}{\mu} (1 + R(\xi)) \exp(i\mu h) J_1(\xi r) u_x(\xi), \tag{3}$$

where $\mu = (k^2 - \xi^2)^{1/2}$, $\mu > 0$ if $\xi < k$, $\Im \mu > 0$ if $\xi > k$. It has been shown in a previous study [13] of an urethane foam with a Poisson ratio $\nu \approx 0.44$ that for a small radial distance $r \approx 1$ cm and a height h of several cm, there is a broad peak in the distribution of \dot{U}_z as a function of frequency related to a compressional resonance of the frame. For r close to 0, $\dot{U}_r(0) = 0$. For $r \approx 20$ cm or more, there is a broad peak in the distribution of \dot{U}_r related to the quarter shear wavelength resonance. The observation of this resonance is less obvious for materials with a small Poisson ratio and a large thickness. Predictions of \dot{U}_r are shown in Figure 2 for a layer of thickness $l = 5$ cm for two Poisson ratios, $\nu = 0.3$ and $\nu = 0.45$ with $h = 2$ cm and $r = 15$ cm. The other parameters that characterize the porous medium are given in Table I. The predicted peak for $\nu = 0.3$ is broadened by the quarter compressional wavelength resonance located closer to the shear resonance. A radial distance r equal or larger than 20 cm is necessary to obtain the maximum for \dot{U}_r at the shear resonance and not at the compressional resonance. Moreover, previous experiments have shown that this peak is often difficult to detect among other peaks probably related to the finite lateral dimensions of the layers. The effect of the finite dimensions can be more important for measurements of the radial velocity than for measurements of the normal velocity because the distance from the source to the point where the velocity is measured must be large for the radial velocity. If the shear resonance cannot be localized with a good

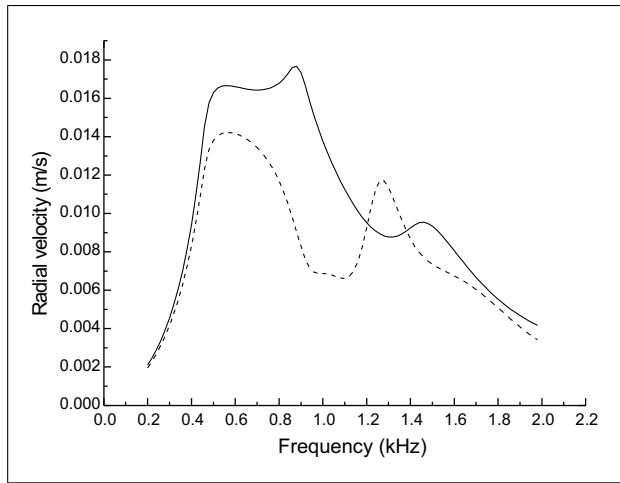


Figure 2. Radial velocity, thickness $l = 5$ cm, $r = 15$ cm, $h = 2$ cm, parameters of Table I except ν , $\nu = 0.3$ —, $\nu = 0.45$ - - - -.

Table I. Parameters for the porous material.

porosity ϕ	0.99
flow resistivity σ [Nm^{-4}s]	12000.
thermal permeability k'_0 [m^2]	1.5×10^{-9}
viscous dimension Λ [μm]	100.
thermal dimension Λ' [μm]	400.
tortuosity α_∞	1.01
density ρ_s [kg/m^3]	9.
shear modulus N [kPa]	$86.(1. + i0.05)$
Poisson ratio $[\nu]$	0.276

precision or is not detectable, another parameter must be measured to evaluate the rigidity parameters in vacuum of the frame considered as an isotropic elastic solid. The chosen parameter is the speed of the Rayleigh wave.

3. Modified Rayleigh wave

As indicated in the Introduction, the modes of the porous structures of sound absorbing media in air are similar to the vibration modes of elastic solids in vacuum having the same rigidity coefficients as the porous structure and the same density. Plane or axi symmetrical surface waves similar to the Rayleigh waves at the surface of an elastic solid can be created at an air-semi infinite porous layer interface [11, 12, 8]. The waves are related to a pole of the reflection coefficient R for a horizontal wave number component ξ_R related to a phase speed of the Rayleigh wave $c_R = \omega/\text{Re}\xi_R$ and a damping $\Im m\xi_R$. The velocity c_R of the compressional wave in the equivalent elastic solid with the shear modulus and the Poisson coefficient of Table I is 176 m/s, and the wavelength at 5 kHz is close to 3.5 cm. The amplitude of the Rayleigh wave inside the medium is noticeable up to a distance to the surface equal to the compressional wavelength. The Rayleigh wave will be slightly modified by the waves reflected at the rigid backing-porous layer interface at 5 kHz for a layer

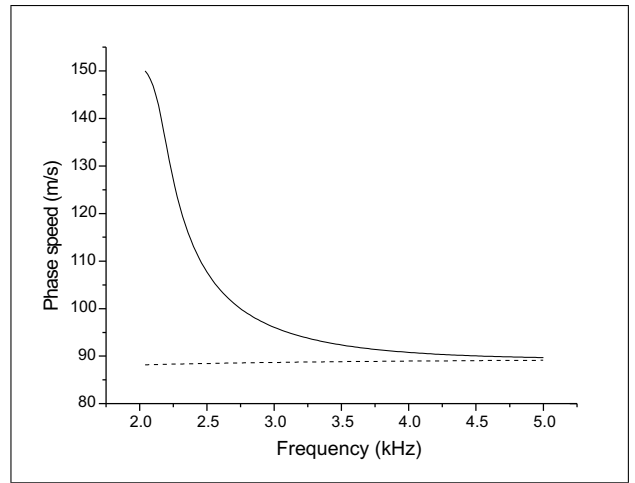


Figure 3. Phase speed $c_R = \omega/\text{Re}\xi_R$ of the modified Rayleigh wave, parameters of Table I except $\nu = 0.3$, thickness $l = 2$ cm —, semi-infinite layer - - - -.

of thickness larger than 3.5 cm. The modifications can be more noticeable for smaller thicknesses and/or lower frequencies. More precisely, with the modeling of reference [13] based on the Biot theory, the Rayleigh wave is not modified if the nine coefficients $r_{i,j}$ that indicate the amplitude, at the air-porous material interface, of the waves reflected at the rigid backing-porous layer interface, fulfil the condition $|r_{i,j}| \ll 1$. The modulus of the coefficients $r_{i,j}$ decreases when the thickness or the frequency increases and their variation is responsible for the dispersion of the Rayleigh waves. The modified velocity and damping can be obtained from ξ_R that can be predicted with an iterative method. The evaluation starts by choosing two ξ , ξ_1 and ξ_2 . Let $\Delta_1(\xi)$ and $\Delta_1(1/R)$ be the variations of ξ and $1/R$ defined by $\Delta_1(\xi) = \xi_2 - \xi_1$, $\Delta_1(1/R) = 1/R(\xi_2) - 1/R(\xi_1)$. The iterative procedure is defined by the general expression

$$\xi_{j+1} = \xi_j - \alpha \left[1/R(\xi_j) \right] \Delta_j(\xi) / \Delta_j(1/R), \quad (4)$$

where α is a real positive number smaller than 1 to avoid a divergence of the series. The successive iterations lead to ξ_R related to $1/R(\xi_R) = 0$. For a layer of finite thickness, there is an infinite number of poles of the reflection coefficient, and iterations must start close to the modified pole. For a layer of thickness $l = 2$ cm, the phase speed is shown in Figure 3 and the damping in Figure 4 as a function of frequency. The material is described by the parameters of Table I, except the Poisson ratio equal to 0.3. Comparisons are performed with the same quantities predicted for a semi-infinite layer. The phase speed and the damping are not noticeably modified for frequencies higher than 4 kHz. Therefore, the coordinates $\text{Re}\xi_R$ and $\text{Im}\xi_R$ of the pole in the complex ξ plane are not noticeably modified at frequencies higher than 4 kHz for a layer of thickness $l = 2$ cm. When frequency decreases, the phase speed increases and the damping becomes much larger than the damping of the non modified Rayleigh wave.

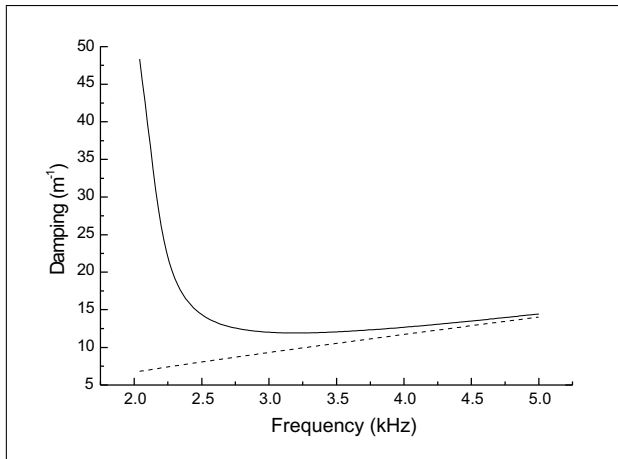


Figure 4. Damping $\Im m \xi_R$ of the modified Rayleigh wave, parameters of Table I except $\nu = 0.3$, thickness $l = 2$ cm —, semi-infinite layer - - - -.

4. Measurements

Measurements have been performed on two layers of melamine of thickness 2 cm and 5 cm and of area 1×1 m². A set of acoustic parameters which gives predictions of the absorption coefficient close to measurements previously performed in a Kundt tube are given in Table I. The location and the width of the predicted peaks are very weakly dependent on the values of the acoustic parameters and mainly depend on the density of the frame ρ_1 , the shear modulus N and the Poisson coefficient ν . The density of the frame is measured and both rigidity coefficients in Table I are chosen to predict Rayleigh wave speeds and peaks of the normal velocities close to the measured ones. To obtain a uniform boundary condition double-faced tape is used to glue the porous layer onto a rigid impervious backing. The point source for the detection of the peaks is a pipe fed by a compression driver and with a microphone located at the end of the tube to provide a reference pressure signal in the frequency domain. The internal diameter of the pipe is equal to 10 mm. The vertical velocity is measured with a laser beam perpendicular to the surface of the layer and for the radial velocity the angle of incidence of the beam is close to 65°. The transfer functions between the velocity signal and the reference pressure signal are shown in Figures 5–8. These transfer functions can be considered as normalized measured velocity distributions. The predicted distributions are also normalized in amplitude with respect to the measured distributions in order to obtain a more precise localization of the peaks. Rayleigh waves are excited by means of a magnetic transducer, fed with a sine burst signal at 4 kHz. Again, a laser vibrometer is used to measure the vertical displacement of the porous layer. Measurement points are located on a radius through the excitation point. The radius is scanned up to 8 cm and with a typical step of 5 mm. The setup is shown in Figure 9. The measured speed of the modified Rayleigh waves is $c_R = 88.1$ m/s for the layer of thickness $l = 5$ cm and $c_R = 89.6$ m/s for the layer of thickness $l = 2$ cm. The pre-

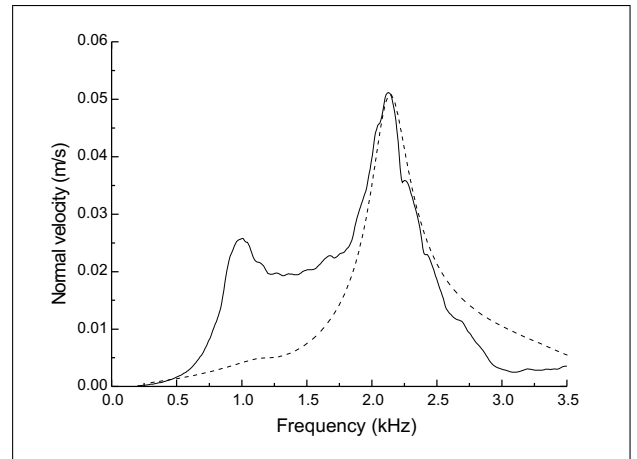


Figure 5. Normal velocity, parameters of Table I, thickness $l = 2$ cm, $h = 4.5$ cm, $r = 0.5$ cm, prediction - - - - measurement —.

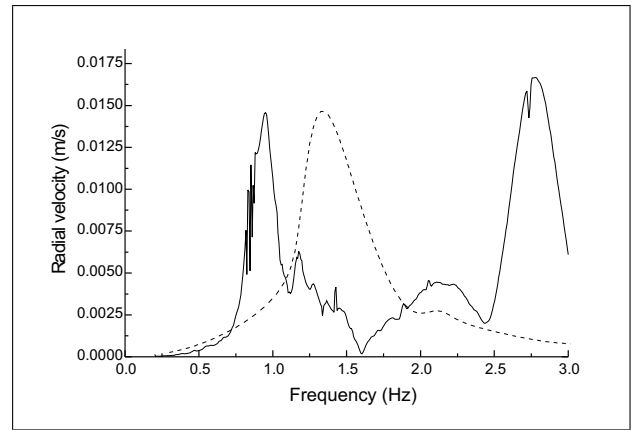


Figure 6. Radial velocity, parameters of Table I, thickness $l = 2$ cm, $h = 4$ cm, $r = 26$ cm, prediction - - - - measurement —.

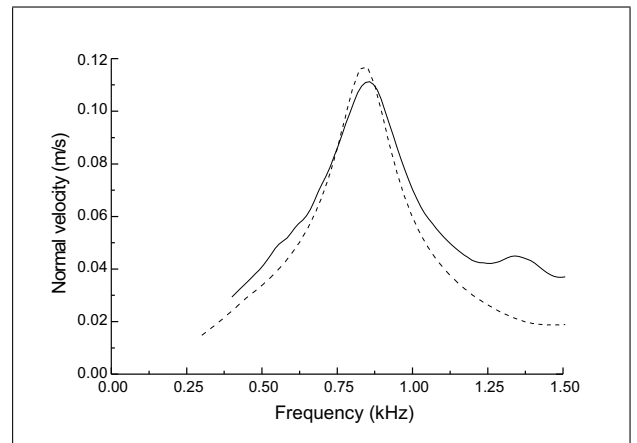


Figure 7. Normal velocity, parameters of Table I, thickness $l = 5$ cm, $h = 1.5$ cm, $r = 0.25$ cm, prediction - - - - measurement —.

dicted phase speeds at 4 kHz, where the wave spectra are peaked, are 88.5 m/s, and 90.3 m/s, respectively. For the layer of thickness $l = 2$ cm, the normalized predicted and measured normal velocities are presented in Figure 5 and

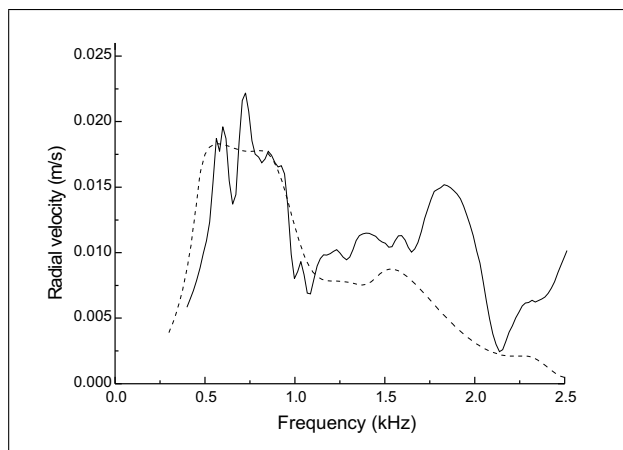


Figure 8. Radial velocity, parameters of Table I, thickness $l = 5$ cm, $h = 1$ cm, $r = 20$ cm, prediction - - - - measurement —.

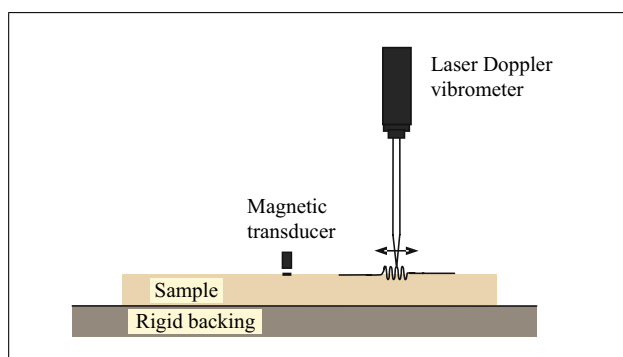


Figure 9. Experimental setup for the generation and detection of Rayleigh waves in a layer of porous material on a rigid backing.

the radial velocities in Figure 6. For the layer of thickness $l = 5$ cm, the normal velocities are presented in Figure 7 and the radial velocities in Figure 8. In Figures 5 and 7 there is a good agreement between the predicted and the measured distributions and the location of the maxima for the peaks related to the quarter compressional wavelength. The Poisson ratio $\nu = 0.276$ provides a ratio between the compressional resonance and the speed of the Rayleigh wave which is in a good agreement for both thicknesses. A previous study [9] of a similar medium has given an order of magnitude of 0.2 for ν and a shear modulus close to 100 kPa at 1 kHz. In reference [9], the shear modulus slightly increases with frequency and the measurements are performed up to 1.3 kHz. The good agreement in the present work between the measured and the predicted frequencies where the maxima of the compressional peaks are located, close to 0.8 kHz and 2.2 kHz respectively, with one set of rigidity coefficients, indicates that the dependence of the frame rigidity on frequency can be neglected. For the thickness $l = 5$ cm, the agreement is poor for the quarter shear wavelength resonance in Figure 8, because the predicted peak is flat and strong variations occur in the related measured transfer function. For the thickness $l = 2$ cm there is no peak in the measured transfer function in Figure 6 at the frequency where the quarter shear wave-

length resonance is predicted. A strong anisotropy of the layer is necessary for the measured peak around 0.8 kHz to be related to a shear resonance. This anisotropy does not appear when quasi-static measurements are performed on different slices of the medium. The peak is probably an effect of the finite lateral dimensions of the sample. Preliminary results obtained with the finite elements method indicate that for materials like melamine where the loss angle is equal to 0.05 or less, reflections on the edges can noticeably modify the radial velocity distribution for layers of lateral dimensions similar to the ones used in measurements. Other possible explanations are a non-uniform boundary condition, due to an imperfect gluing, or inhomogeneities of the material.

5. Conclusion

The Poisson ratio and the shear modulus of a melamine foam have been evaluated at audible frequencies from a measurement of the phase velocity of the Rayleigh waves modified by the finite thickness of the layers and from the observation of the compressional quarter wavelength resonance of the porous frame. Measurements have been performed on two porous layers of different thicknesses bonded on a rigid impervious backing. The Rayleigh wave is very slightly modified, even for the sample with the smallest thickness. The compressional resonance is related to a peak of the vertical velocity of the frame induced at the surface of the layer by a point source in air. Predictions obtained for both thicknesses with one set of rigidity coefficients are in a good agreement with the measurements for the compression peaks and the speed of the modified Rayleigh waves. In a previous work performed on a urethane foam with a larger Poisson ratio, the shear modulus was evaluated from the localization of the quarter shear wavelength resonance with a peak of the radial velocity. For the melamine samples studied, the measurement of the radial velocity of the frame does not provide a very precise localization of the quarter shear wavelength resonance for the thickest layer, and for the thinnest layer, there was no peak detected close to the predicted one. Due to the closeness of the shear resonance and the compressional resonance, the radial velocity cannot be used to localize the shear resonance.

Appendix

Prediction of the parameters of the Biot theory

The Biot theory, with the formalism developed in reference [3] has been used to predict the surface impedance with the model by Johnson *et al.* [14] for the viscous and inertial interaction, and the model by Lafarge [15] for the bulk modulus of air. The Biot elasticity coefficients P , Q , and R , with the simplifications suggested in reference [3] are given by

$$P = \frac{4}{3}N + K_b + \frac{(1 - \phi)^2}{\phi} K_f, \quad (\text{A1})$$

$$Q = K_f(1 - \phi), \quad (A2)$$

$$R = \phi K_f, \quad (A3)$$

$$K_b = \frac{2}{3}N(1 + \nu)/(1 - 2\nu), \quad (A4)$$

where K_b is the bulk modulus of the frame, N is the shear modulus, ν the Poisson ratio, and ϕ the porosity. The bulk modulus K_f of the air saturating the porous frame is given in the present work by

$$K_f = \frac{K_a}{\beta}, \quad (A5)$$

where K_a is the adiabatic bulk modulus of air and β is given by

$$\beta = \gamma - (\gamma - 1) \left[1 + \frac{1}{-i\tilde{\omega}'} \sqrt{1 - \frac{M'}{2}i\tilde{\omega}'} \right]^{-1}, \quad (A6)$$

$$\tilde{\omega}' = \frac{\rho_0 \text{Pr} \omega k'_0}{\eta \phi}, \quad (A7)$$

$$M' = \frac{8k'_0}{\phi \Lambda^2}. \quad (A8)$$

In these equations, η is the viscosity and ρ_0 is the density of air, γ is the ratio of the specific heats and Pr is the Prandtl number, k'_0 is the thermal permeability and Λ is the thermal characteristic dimension of the porous frame.

The renormalized densities of the Biot theory $\tilde{\rho}_{11}$, $\tilde{\rho}_{22}$, and $\tilde{\rho}_{12}$ are given by

$$\tilde{\rho}_{11} = \rho_1 + \rho_a - ib, \quad (A9)$$

$$\tilde{\rho}_{12} = -\rho_a + ib, \quad (A10)$$

$$\tilde{\rho}_{22} = \phi \rho_0 + \rho_a - ib. \quad (A11)$$

The coefficient b related to the viscous and the inertial interaction is given in the present work by

$$b = -\frac{\sigma}{\omega} \phi^2 G_j(\omega), \quad (A12)$$

$$G_j(\omega) = \sqrt{1 - \frac{4i\alpha_\infty^2 \eta \rho_0 \omega}{\sigma^2 \Lambda^2 \phi^2}}, \quad (A13)$$

where α_∞ is the tortuosity, σ is the flow resistivity, and Λ is the characteristic viscous dimension. The added density ρ_a is given by

$$\rho_a = \rho_0 \phi (\alpha_\infty - 1). \quad (A14)$$

The wave numbers k_1 and k_2 for both Biot compressional waves, and k_3 for the Biot shear wave, are given by

$$k_{1,2}^2 = \frac{\omega^2}{2(PR - Q^2)} \cdot [P\tilde{\rho}_{22} + R\tilde{\rho}_{11} - 2Q\tilde{\rho}_{12} \pm \sqrt{\Delta}], \quad (A15)$$

$$k_3^2 = \frac{\omega^2}{N} \left[\frac{\tilde{\rho}_{11}\tilde{\rho}_{22} - \tilde{\rho}_{12}^2}{\tilde{\rho}_{22}} \right], \quad (A16)$$

$$\Delta = (P\tilde{\rho}_{22} + R\tilde{\rho}_{11} - 2Q\tilde{\rho}_{12})^2 - 4(PR - Q^2)(\tilde{\rho}_{11}\tilde{\rho}_{22} - \tilde{\rho}_{12}^2). \quad (A17)$$

The coefficients μ which give the ratio of the air velocity components to the frame velocity components are given by

$$\mu_{1,2} = \frac{Pk_{1,2}^2 - \omega^2 \tilde{\rho}_{11}}{\omega^2 \tilde{\rho}_{12} - Qk_{1,2}^2}. \quad (A18)$$

$$\mu_3 = -\tilde{\rho}_{12}/\tilde{\rho}_{22}. \quad (A19)$$

Acknowledgement

The second author (L. B.) thanks the Institute for the Promotion of Innovation by Science and Technology in Flanders for the provided funding.

References

- [1] M. A. Biot: Theory of propagation of elastic waves in a fluid-saturated porous solid. *J. Acoust. Soc. Am.* **28** (1956) 168–191.
- [2] M. A. Biot, D. G. Willis: The elastic coefficients of the theory of consolidation. *J. Appl. Mechanics* **24** (1957) 594–601.
- [3] J. F. Allard: Propagation of sound in porous media. Modelling sound absorbing materials. Elsevier, London, 1993.
- [4] T. Pritz: Measurement methods of complex Poisson's ratio of viscoelastic materials. *Appl. Acoust.* **60** (2000) 279–292.
- [5] M. Melon, M. Mariez, C. Ayrault, S. Sahraoui: Acoustical and mechanical characterization of anisotropic open-cell foams. *J. Acoust. Soc. Am.* **104** (1998) 2622–2627.
- [6] J. Park: Measurement of the frame acoustic properties of porous and granular materials. *J. Acoust. Soc. Am.* **118** (2005) 3483–3490.
- [7] V. Tarnow: Dynamic measurements of the elastic constants of glass wool. *J. Acoust. Soc. Am.* **118** (2005) 3672–3678.
- [8] J. F. Allard, G. Jansens, G. Vermeir, W. Lauriks: Frame-borne surface waves in air-saturated porous media. *J. Acoust. Soc. Am.* **111** (2002) 690–696.
- [9] L. Boeckx, P. Leclaire, P. Khurana, C. Glorieux, W. Lauriks, J. F. Allard: Investigation of the phase velocity of guided acoustic waves in soft porous layers. *J. Acoust. Soc. Am.* **117** (2005) 545–554.
- [10] L. Boeckx, P. Leclaire, P. Khurana, C. Glorieux, W. Lauriks, J. F. Allard: Guided waves at audible frequencies in poroelastic layers in the Lamb conditions. *J. Appl. Phys.* **97** (2005) 094911.
- [11] K. Attenborough, T. L. Richards: Solid particle motion induced by a point source above a poroelastic half-space. *J. Acoust. Soc. Am.* **86** (1989) 1085–1089.
- [12] K. Attenborough, Y. Chen: Surface waves at an interface between air and an air-filled poroelastic ground. *J. Acoust. Soc. Am.* **87** (1990) 1010–1016.
- [13] J. F. Allard, B. Brouard, N. Atalla, S. Ghinet: Excitation of soft porous frames resonances and evaluation of the rigidity coefficients. *J. Acoust. Soc. Am.* **121** (2007) 78–84.
- [14] D. L. Johnson, J. Koplik, R. Dashen: Theory of dynamic permeability and tortuosity in fluid-saturated porous media. *J. Fluid Mech.* **176** (1987) 379–402.
- [15] D. Lafarge, P. Lemarinier, J. F. Allard, V. Tarnow: Dynamic compressibility of air in porous structures at audible frequencies. *J. Acoust. Soc. Am.* **102** (1997) 1995–2006.
- [16] L. M. Brekhovskikh, O. A. Godin: Acoustics of layered media II, Point source and bounded beams. Springer series on wave phenomena. Springer, New York, 1992.